Chemistry
A European
Journal

Chemistry Europe
European Chemical Societies Publishing

Accepted Article

Title: DNA-Triggered Enhancement of Singlet Oxygen Production by Pyridinium Alkynylanthracenes

Authors: Torsten Linker, Werner Fudickar, Marcel Bauch, and Heiko Ihmels

To be cited as: *Chem. Eur. J.* 10.1002/chem.202101918

Link to VoR: https://doi.org/10.1002/chem.202101918

WILEY-VCH

10.1002/chem.202101918

WILEY-VCH

FULL PAPER

DNA-Triggered Enhancement of Singlet Oxygen Production by Pyridinium Alkynylanthracenes

Werner Fudickar,[a] Marcel Bauch,[a] Heiko Ihmels,[b] and Torsten Linker*[a]

[a] Dr. W. Fudickar
Dr. M. Bauch
Prof. Dr. T. Linker
Department of Chemistry
University of Potsdam
Karl-Liebknecht-Str. 24-25
14476 Potsdam
E-mail: linker@uni-potsdam.de

[b] Prof. Dr. H. Ihmels
Department of Chemistry
University of Siegen
Adolf-Reichwein-Str. 2
57068 Siegen

Supporting information for this article is given via a link at the end of the document.

Abstract: There is an ongoing interest in $^1O_2$ sensitizers, whose activity is selectively controlled by their interaction with DNA. To this end, we synthesized three isomeric pyridinium alkynylanthracenes **2*o*–*p*** and a water-soluble trapping reagent for $^1O_2$. In water and in the absence of DNA, these dyes show a poor efficiency to sensitize the photooxygenation of the trapping reagent as they decompose due to electron transfer processes. In contrast, in the presence of DNA $^1O_2$ is generated from the excited DNA-bound ligand. The interactions of **2*o*–*p*** with DNA were investigated by thermal DNA melting studies, UV/vis and fluorescence spectroscopy, and linear and circular dichroism spectroscopy. Our studies revealed an intercalative binding with an orientation of the long pyridyl-alkynyl axis parallel to the main axis of the DNA base pairs. In the presence of poly(dA:dT), all three isomers show an enhanced formation of singlet oxygen, as indicated by the reaction of the latter with the trapping reagent. With green light irradiation of isomer **2*o*** in poly(dA:dT), the conversion rate of the trapping reagent is enhanced by a factor >10. The formation of $^1O_2$ was confirmed by control experiments under anaerobic conditions, in deuterated solvents, or by addition of $^1O_2$ quenchers. When bound to poly(dG:dC), the opposite effect was observed only for isomers **2*o*** and **2*m***, namley the trapping reagent reacted significantly slower. Overall, we showed that pyridinium alkynylanthracenes are very useful intercalators, that exhibit an enhanced photochemical $^1O_2$ generation in the DNA-bound state.

Introduction

A vast number of dyes has been used as sensitizer in photodynamic therapy (PDT) with the intention to elicit cell-death.[1–6] In PDT, malignant cells are destroyed by virtue of reactive oxygen species (ROS), which are generated upon excitation of the dye (Figure 1).[7–9] Two key processes, generally denoted as Type I and Type II, start from the excited triplet state T_n of the sensitizer after intersystem crossing (ISC). In a Type I reaction, electron transfer (ET) processes take place, from which ROS such as superoxide or hydroxyl radicals are formed, whereas in a Type II process, energy from the T_n state is transferred to oxygen in the triplet ground state, generating singlet oxygen ($^1O_2$). Both processes are essential in the photosensitized cell-destruction.

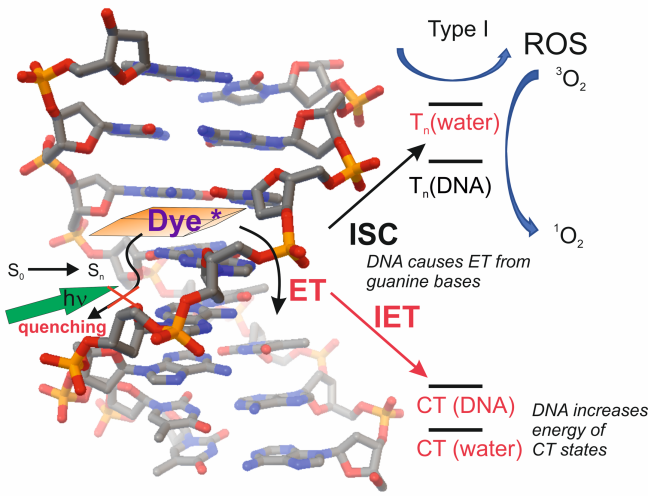

Figure 1. Schematic illustration of the photophysical processes following excitation of a photosensitizing, DNA-bound dye: The ISC to a T_n, from which ROS can be generated, are competing with (i) intramolecular electron transfer (IET) to CT transitions, (ii) quenching by vibration or rotation of bonds, and (iii) ET from guanine bases.

A general drawback of PDT is the unselective generation of ROS, which operate differently, and the lack of control over their location in the tissue. To cope with these shortcomings, the ability of certain dyes to selectively bind to DNA has been exploited.[10–12] In this approach, it is proposed that the local ROS generation in the close proximity of the DNA-bound dye would cause more specific damage to the nucleic acid, such as oxidation of guanine bases or DNA strand breaks.[13] Along these lines, the improvement of selectivity was realized by the identification of organic dyes which become photophysically active only upon interaction with DNA.[14] Hence, Hirakawa *et al* have found that the alkaloids berberine and palmatine, which bind to DNA with several distinct binding modes, generate $^1O_2$ only in the presence

10.1002/chem.202101918

of DNA.[15–17] They ascribed this dependence on the environment to the switching of the deactivation of the excited state S_1 from charge transfer (CT) to an ISC to the T_n state because the energy of the CT state of the DNA-bound ligand increases and exceeds the one of the T_n state (Figure 1). Enhancement of $^1O_2$ production has also been observed for chalcogenopyrillium dyes, as their interaction with DNA caused a restriction of molecular flexibility, which is an important channel of quenching.[18] As a result, the increased lifetime of the excited state enables ICT and $^1O_2$ generation in the presence of the DNA ligand. And in addition, the short lifetime of $^1O_2$ and thus its limited radius of action also contributes to a locally restricted DNA damage.[19,20]

On the other hand, the contrary phenomenon, namely the decreasing ability to generate $^1O_2$ is known for DNA-bound photosensitizers. Thus, intercalated tetracationic porphyrins have significantly smaller $^1O_2$-quantum yields (Φ_Δ) than their free forms.[21,22] In this case, the effect is caused by quenching of the S_1 state of the sensitizer by a reversible ET from guanine residues (Figure 1). To summarize, the three important processes, which contribute to the yield of $^1O_2$ production, are shown in Figure 1.

An additional important aspect in the prediction of the efficiency of the $^1O_2$ generation was recently addressed, which pointed at the impact of DNA on the rate of ISC.[23] Thus, DNA stabilizes the intercalator triplet state involved in the ISC relative to an aqueous environment and opens a new pathway of electronic spin-orbit coupling for a faster ISC. Based on these observations, we concluded that the following parameters are decisive for a $^1O_2$ sensitizer, whose efficiency is enhanced in the presence of DNA: (i) The DNA-mediated control over structural separation of electron-rich and electron-poor moieties allowing intramolecular electron transfer (IET) processes, (ii) a flexible unit, e. g. a rotating bond, contributing to torsional relaxation, and (iii) control over the energy of the T_n state that is responsible for eliciting Type I/II reactions. In addition, in order to bind to DNA, structural features such as positive charges, and a molecular shape that fits the binding sites are mandatory.[24–31]

We have investigated the reactions of anthracenes with $^1O_2$,[32–34] and recently reported on a series of *N*-methylated derivatives of dipyridylanthracenes **1*o*–*p***, which associate with DNA as groove binders (Figure 2).[35] However, these compounds showed more activity to produce $^1O_2$ in their free form compared with the one of their DNA-bound state. We ascribed this behavior to the lack of DNA-mediated control over the above-mentioned features due to the hindered rotation of the pyridinium groups. In addition, these derivatives did not show a tendency to interact with GC-rich polynucleotides, a typical feature of groove binders. To address these missing features, we synthesized the three isomeric pyridinium alkynylanthracenes **2*o*–*p*** (Figure 2). We anticipated that these compounds should offer an additional channel for quenching of the excited state by free rotation about the alkyne C–C single bonds to accomplish full conjugation along the anthracene short axis and thereby interrupt IET. In addition, their planar structure should enable the intercalation into DNA. Herein, we present our studies of the interaction of these compounds with calf thymus (ct) DNA and the polynucleotides poly(dA:dT) and poly(dG:dC), and we demonstrate that these compounds act as $^1O_2$ sensitizers, whose efficiency is controlled by the interaction with the polynucleotides.

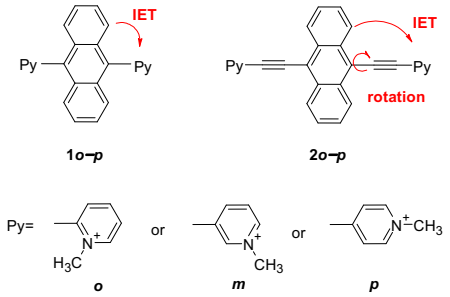

Figure 2. Structures of pyridinium anthracenes **1** and pyridinium alkynylanthracenes **2**.

Results and Discussion

Synthesis of the pyridinium alkynylanthracenes. In analogy to an established procedure,[36] Sonogashira coupling between alkynylpyridines **3*o*–*p***[37] and dibromoanthracene **4** afforded 9,10-bis(pyridylalkynyl)-anthracenes **5*o*–*p***, which were methylated by subsequent reaction with dimethyl sulfate to give the methyl pyridinium alkynylanthracenes **2*o*–*p*** in 70–80% overall yield (Scheme 1, Experimental Section).

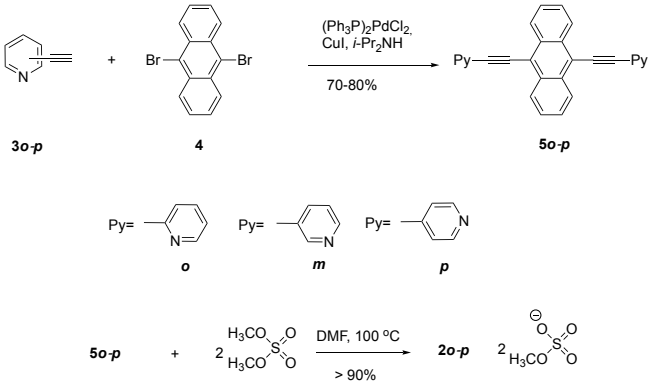

Scheme 1. Synthesis of the pyridinium alkynylanthracenes **2*o*–*p*.**

Photochemical properties of the pyridinium alkynylanthracenes in water. To assess the suitability of the anthracene derivatives **2*o*–*p*** as photosensitizers, we sought for a charge-neutral water-soluble probe, since positive or negative charges could cause interference either with the negatively charged phosphate groups of DNA, or the positively charged pyridinium groups of the sensitizer. For that purpose, we recently synthesized carbohydrate-substituted naphthalenes.[38] However, to follow the response of such probes by UV/vis spectroscopy, we replaced the naphthalene with an anthracene core, whose absorption bands are shifted to longer wavelength in the visible range. By using the same synthetic route as for the naphthalene derivative, we started from anthraquinone (**6**) as precursor, which was reduced to anthrahydroquinone (**7**), and coupled with the imidate (**8**)[39] to obtain 9,10-bis-*O*-*β*-D-glycosylanthracene (**GLYANT**) in good overall yield (Scheme 2). Upon irradiation in the presence of the known photosensitizer methylene blue under oxygen atmosphere, this water-soluble probe reacted with the generated $^1O_2$ quantitatively to its corresponding endoperoxide

10.1002/chem.202101918

GLYANTO2. The reaction was easily followed by the decrease of the absorbance maxima of **GLYANT** between 350 and 400 nm.

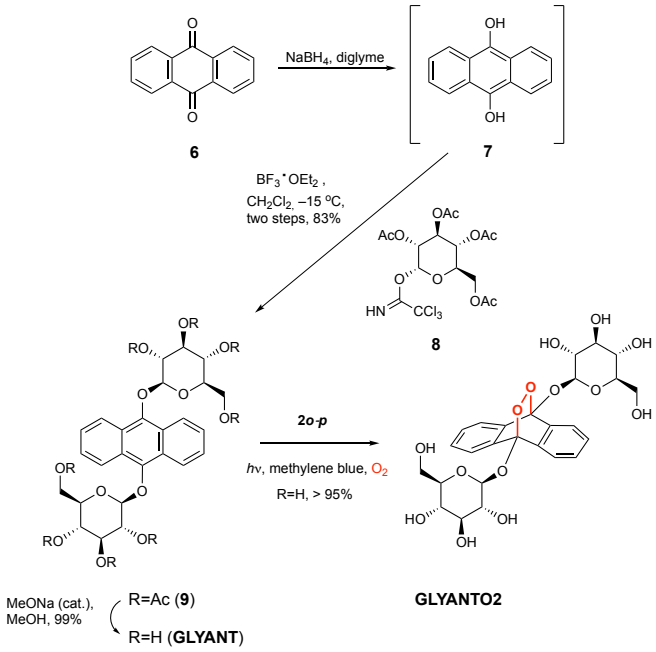

Scheme 2. Synthesis of the trapping reagent **GLYANT** and its reaction to the endoperoxide **GLYANTO2** upon irradiation in the presence of the dyes **2*o*–*p***.

The response of the trapping reagent **GLYANT** on irradiation of the sensitizers **2*o*–*p*** was followed by irradiation of mixtures of equimolar amounts of **GLYANT** and **2*o*–*p*** with LED-light at a wavelength of 485 nm. At this wavelength, all three sensitizers absorb strongly, whereas the trapping reagent is transparent and showed no photoreaction in the absence of the photosensitizers. In contrast, the absorption bands between 350–400 nm, indicative of **GLYANT**, decreased during the course of the photoreaction of **2*o*–*p*** (Figure 3a–c). A significantly faster decrease was observed for the two isomers **2*o*** and **2*p*** as compared with the *meta* isomer **2*m***. This reaction accelerated by a factor greater than 10, when D_2O was used instead of H_2O as solvent (shown for isomer **2*m*** in Figure 3d). This observation accounts for a reaction based on $^1O_2$, since the lifetime of this reactive species is prolonged from 3 µs in H_2O to 67 µs in D_2O.[40]

However, a bleaching of the dyes occurred as well, which was discerned by the decrease of their absorbance maxima between 450–500 nm. Bleaching was fast for isomer **2*m***, proceeded slower for **2*p***, but almost no bleaching occurred for the *ortho* derivative **2*o***. To unravel the origin of this photoinduced decomposition, we irradiated **2*o*–*p*** with red light in the presence of the $^1O_2$ sensitizer methylene blue, but observed no changes in the UV spectra. Thus, the anthracene core of the sensitizers is inert towards $^1O_2$. In contrast, irradiation of the sensitizers with 485 nm blue light under anaerobic conditions showed bleaching, a slow process observed for the *ortho* and *para* isomers and a very fast one for the *meta* derivative (see Supporting Information Figure S1). Irradiation under anaerobic conditions in the presence of the trapping reagent showed also a decrease of the absorption bands of the latter, which proceeded for **2*o*** and **2*m*** almost within the same time range as under oxygen atmosphere, but significantly slower for **2*p***.

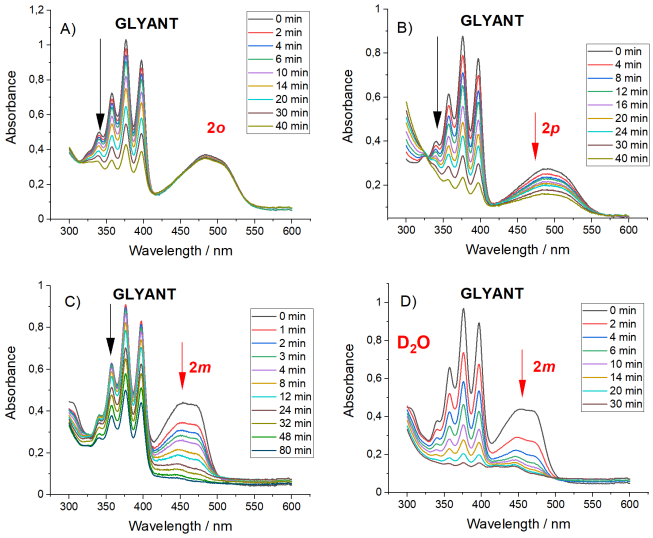

Figure 3. Singlet oxygen generation by pyridinium alkynylanthracenes **2*o*–*p*** in water monitored by the decrease of the absorption bands of **GLYANT**. A) Sensitizer **2*o***, B) **2*p***, C) **2*m***, and D) **2*m*** in D_2O.

These observations led to the conclusion, that after excitation and ISC into the T_n state, $^1O_2$ generation (Type II) competes with ET processes, where both intra- and intermolecular reactions can occur. Such an ET is possible if the free enthalpy change ΔG becomes negative (eq. 1).[41,42]

$$\Delta G = E_{ox} - E_{red} - \Delta E_{0,0} \qquad \text{(eq 1)}$$

Here, E_{ox} is the oxidation potential of the donor, E_{red} is the reduction potential of the acceptor and $\Delta E_{0,0}$ is the energy of the 0-0 transition from the ground state to the first excited state (see Supporting Information for its determination). E_{red} was determined by cyclic voltammetry, where one reversible and an additional irreversible reduction peak were found for isomers **2*o*** and **2*p***, whereas no waves were observed for the *meta* isomer (see Figure S2, Supporting Information). From these data, the oxidation potential of the dye in its excited state was derived as 1.71 V for **2*o*** and 1.55 V for **2*p***. These high oxidation potentials are in accordance with the observation, that excited **2*o*** and ***p*** react in an ET reaction with **GLYANT** with no oxygen involved. It is known that anthracenes with electron donating substituents at the 9,10 position are oxidized at low potentials (< 1 V) upon formation of radical cations stabilized by their substituents.[43] In the case of the *meta* isomer **2*m***, such an ET may involve also the inherent anthracene unit because of the cross-conjugation with the electron withdrawing pyridinium moiety. This cross-conjugation explains also the absence of reduction peaks in the cyclic voltammogram of **2*m***.

Considering that equimolar amounts of sensitizer and probe have been used, the fast bleaching as observed for **2*m*** and **2*p*** makes these isomers unsuitable for application as Type II photosensitizers in their free forms. Nevertheless, the interaction with DNA may eradicate this deficiency.

10.1002/chem.202101918

Interaction of the pyridinium alkynylanthracenes with DNA. To assess the interaction of derivatives **2*o*–*p*** with DNA, melting and titration studies were first undertaken with ct-DNA (Supporting Information). The melting temperature of DNA, T_m, was determined by measurement of the absorption of ct-DNA at 260 nm at increasing temperatures between 40 °C and 100 °C.[44] Upon addition of the pyridinium alkynylanthracenes **2*o*–*p*** at a ratio ligand/bp = 1:2, the melting temperature of ct DNA (T_m = 73 °C) significantly increased by 11 °C with **2*p*** and by 16 °C with **2*m*** (Figure 4). The rise of the T_m values is inferred to a thermodynamic stabilization of the DNA helix, which is known to be caused by association with a ligand.[45–47] With the *ortho* isomer **2*o*** no increase of T_m was observed.

In aqueous solution, UV/vis spectra of the three isomers **2*o*–*p*** showed one broad absorption band in the region between 450–550 nm without a vibrational fine structure (Figure 5). Such broadening is often a result of aggregation, which may also be the case with **2*o*–*p*** due to their planar structures and potential hydrophobic nature.[48] The absorption maximum of the *meta* isomer **2*m*** appeared at significantly lower wavelength, possibly because the acene unit is not in conjugation with the pyridinium groups. Upon titration of the alkynylanthracenes with ct-DNA, the absorption bands showed a bathochromic shift and their intensities decreased (Figure 5). At the early stages of the titration, isosbestic points were observed pointing at one distinctive binding mode. After a ratio of bp/ligand~2:1 (bp = base pairs) was reached, isosbestic points vanished and spectra of isomers **2*o*** and **2*m*** became structured with distinct maxima. Since such spectral changes could also result from disaggregation, we measured spectra at different concentrations, solvents, and temperatures (see Supporting Information Figures S4 and S5). No noticeable changes were observed upon dilution, increased temperatures or change to organic solvents such as ethanol, which confirmed that disaggregation did not contribute to the changes resulting from DNA titration.

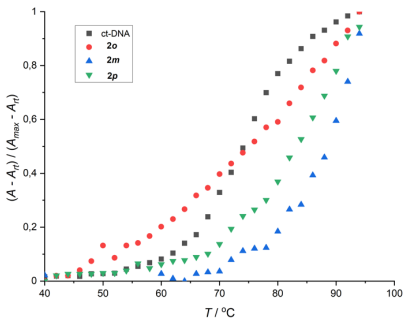

Figure 4. Melting curves of ct-DNA (4 x 10^{-5} M, in base pairs) in the presence of pyridinium alkynylanthracenes **2*o*–*p*** (2 x 10^{-5} M). *A* is the measured absorbance, A_{rt} the absorbance at room temperature and A_{max} the absorbance at the maximum temperature (Supporting Information).

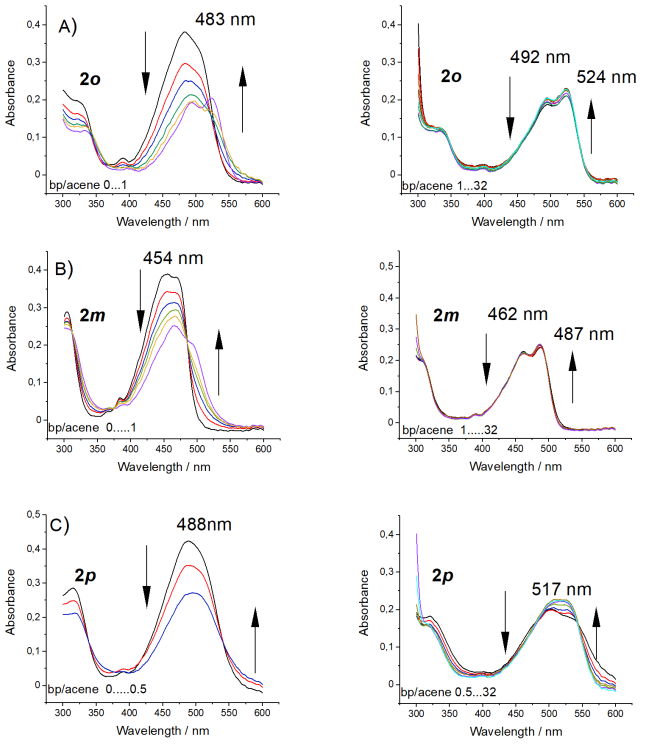

Figure 5. Photometric titration of pyridinium alkynylanthracenes **2*o*–*p*** (2 x 10^{-5} M) with ct-DNA from a ratio bp/ligand = 0 to 32. The left column indicates the early stage of titration with low DNA content, the right column shows the late stage with large content of DNA.

The spectral changes can be attributed to both, groove binding and intercalation.[49] Since association with DNA would interrupt aggregation, the vibrational fine structure becomes more pronounced.

Further insight into the binding modes of ligands **2*o*–*p*** with DNA was gained by flow linear dichroism (LD) and circular dichroism (CD) spectroscopy. The LD spectra showed clear negative LD bands in the absorption range of the ligands between 400 and 550 nm, that intensified with increasing ligand-DNA ratio (Figure 6a–c). These negative bands indicate that the transition dipole moments of the ligands have essentially the same orientation relative to the applied hydrodynamic field as the nucleic bases, which usually indicates an intercalative binding mode.[50,51] In the CD spectra of solutions of anthracenes **2*o*–*p*** with ct-DNA (ratio bp/ligand = 4:1), a strong negative band between 300 and 350 nm (–6 to –14 mdeg) appeared (Figure 6d–f). For isomers **2*o*** and **2*m*** the signs became positive at wavelengths >350 nm. In contrast, the CD band of **2*p*** has a sigmoidal shape and becomes negative in the region >450 nm, where the dye absorbs. These observations suggest overlapping transitions of differently associating ligands **2*p***.

To summarize, increased T_m values, changes in UV/vis absorption spectra and the effects in LD and CD spectra confirm that pyridinium alkynylanthracenes **2*o*–*p*** bind to DNA, preferentially by intercalation, but also additional binding modes are indicated. However, for a better understanding of the operative binding modes, the role of the nucleotide bases AT *versus* GC has also to be considered. We therefore continued our studies with the polynucleotides poly(dA:dT) and poly(dG:dC).

10.1002/chem.202101918

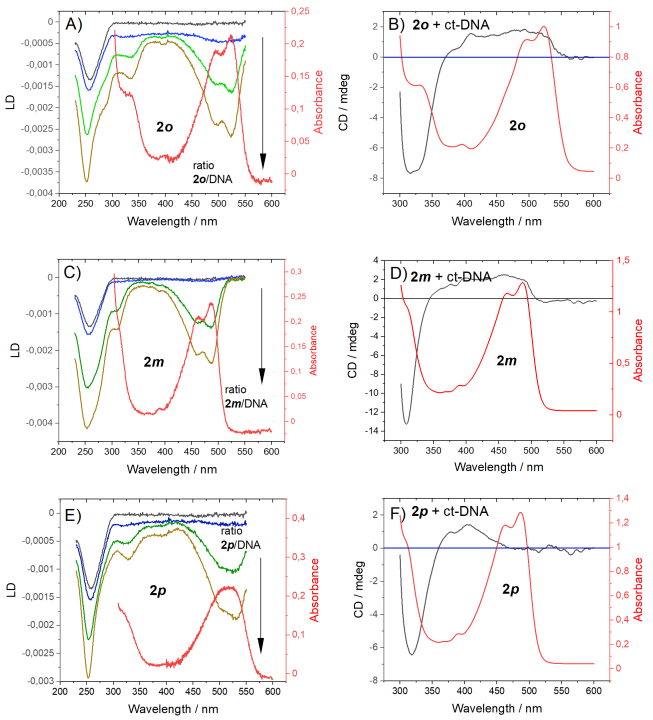

Figure 6. LD and CD spectra of pyridinium alkynylanthracenes ***2o–p*** in the presence of ct-DNA. A-C) LD spectra at different ligand-to-base pair ratios (black: only ct-DNA, blue: 1:1, green: 10:1, brown: 1:20). The red curve shows the absorption spectrum of the DNA-bound ligand. D–F) CD spectra of ct-DNA (black).

The strongly increased melting temperatures of DNA in the presence of the ligand and the negative LD signals of the DNA-bound ligand point to an intercalative binding mode.

During titration of ligands ***2o–p*** with poly(dA:dT) and poly(dG:dC), isosbestic points were found for ***2o*** and ***2p*** pointing at one major binding mode (Figure S6, Supporting Information). With the aim to predict the orientation of the intercalated anthracenes ***2o–p***, we measured their CD spectra with poly(dA:dT) and poly(dG:dC) (ratio bp/ligand = 2:1) (Figure 7). The absorption spectra indicate three distinctive chromophores, for which individual CD signal patterns were found. The first band is located in the range between 300 and 350 nm with strong negative sign in the CD, followed by a weaker absorption with positive CD between 350–450 nm and finally at > 450 nm, where the sign becomes positive.[52]

To assign the ICD bands of the DNA-bound ligands to electronic transitions, we performed density functional theory (DFT) calculations. Accordingly, structures were optimized by DFT-B3LYP/6-31G* followed by time dependent DFT (TDDFT) calculations. By using the PBE0 functional, a good match with experimental data was accomplished (Table S1, Supporting Information).

For the *para* derivative ***2p***, for example, the band with a maximum at 320 nm matches with the S0→S6 transition with a calculated wavelength of 350 nm. Its dipole vector is aligned parallel to the anthracene short axis, which connects the two alkynyl substituents (Figure 8). Assuming an intercalative mode, as proven by the increased T_m and by negative LD bands, the orientation of the intercalator can be deduced roughly from the sign of the corresponding ICD signal. Thus, the negative ICD for ***2p*** at 320 nm arises from a parallel orientation of this transition dipole vector with respect to the long axes of the base pairs, which constitute the intercalation pocked. This relation is also fulfilled with S0→S3 transition with a calculated absorption at 380 nm, which is orthogonal to the anthracene short axis since the CD has a positive sign in this region. In contrast to this new class of DNA binding pyridinium alkynylanthracenes, most hitherto known anthracene intercalators show an orientation with the long wavelength chromophore oriented parallel to the base pairs.[53,54]

For long-wavelength S0→S1 transitions, the spectra have a bisignate shape in the respective wavelength region, which rather points at intermolecular exciton coupling due to coupling between differently binding ligands. One exception is observed with ***2p***/poly(dG:dC), where the sign is negative. Since GC sites exhibt an additional hydrogen bond, this effect could originate from a rejection of the ligand binding to other sites except the intercalation pocket.

In order to confirm the proposed orientation of the ligand in the binding site, we also performed docking calculations of gas-phase optimized structures with the AutoDock Vina program (see Supporting Information).[55] As suitable host model we used solid-state data obtained by X-ray diffraction analysis of a $(CGATCG)_2$ hexamer with two intercalation pockets between the outer C and G bases (Supporting Information, Section 12). As shown in Figure 9, several docking conformations were found, which match with the orientation of the pyridinium alkynylanthracenes aligned parallel to the long axis of the base pairs. These comprehensive studies revealed that pyridinium alkynylanthracenes intercalate into both AT and GC base pairs along the DNA long axis.

10.1002/chem.202101918

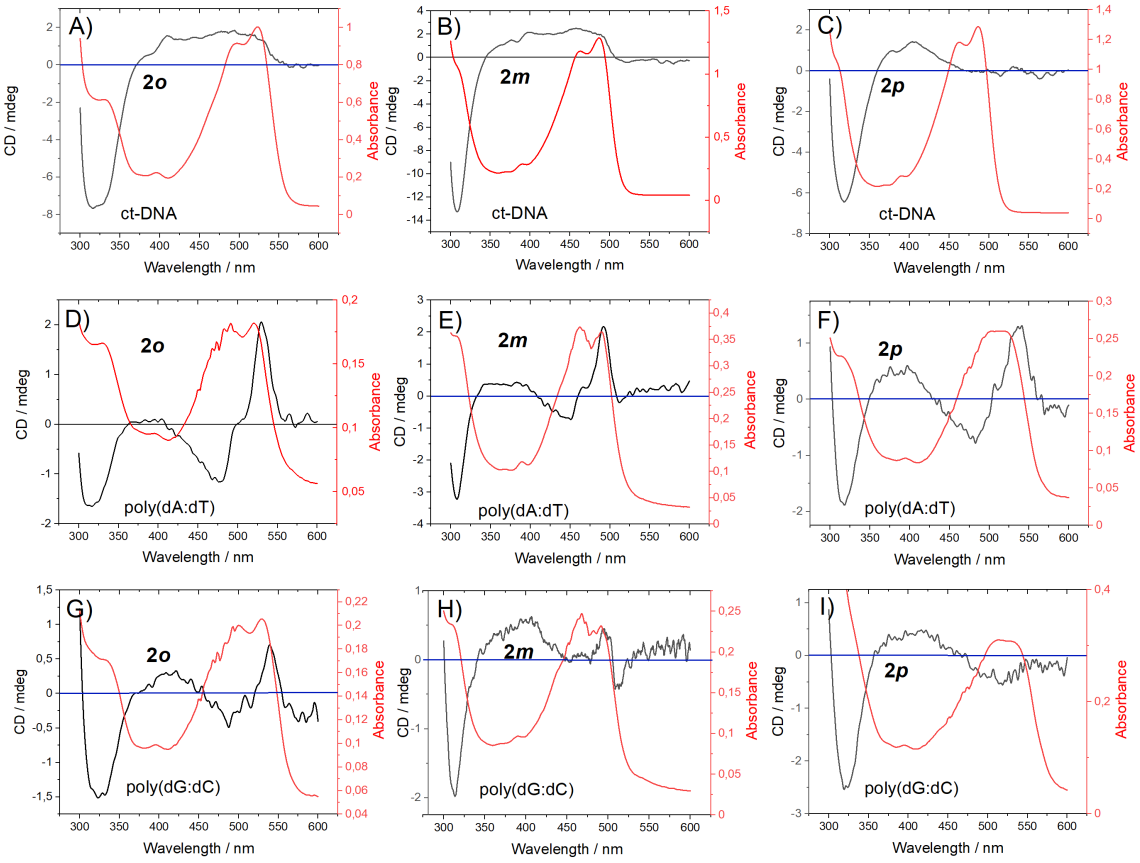

Figure 7. CD spectra of pyridinium alkynylanthracenes **2*o*–*p*** in the presence of DNA. A)–C): **2*o*–*p*** (1 x 10^{-4} M) and ct-DNA (4 x 10^{-4} M); D)–F) **2*o*–*p*** (2 x 10^{-5} M) and poly(dA:dT) (4 x 10^{-5} M); **2*o*–*p*** (2 x 10^{-5} M) and poly(dG:dC) (4 x 10^{-5} M).

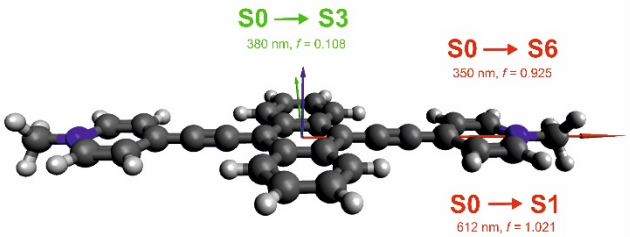

Figure 8. Allowed electronic transitions and dipole moments of pyridinium alkynylanthracene **2*p***.

Excited state properties of the pyridinium alkynylanthracenes in the presence of DNA. We next addressed the effects on excited states arising from this binding mode. Titration of the three isomers with ct-DNA caused also significant changes in the fluorescence spectra of **2*o*–*p*** (Figure 10 and Figures S7–S9, Supporting Information). The strong emission of the *ortho* isomer **2*o*** (Φ_{fl} = 0.64) decreased upon addition of ct-DNA, whereas the non-emissive *meta* derivative **2*m*** (Φ_{fl} < 0.01) became strongly fluorescent in the presence of ct-DNA. Finally, on addition of DNA to **2*p*** (free form, Φ_{fl} = 0.03), the emission initially decreased until a ratio bp/ligand = 2 was reached and then it increased with an excess of DNA. As we have ruled out disaggregation as described above, the enhancement of fluorescence of **2*m*** may originate from the reduction of molecular vibrations and rotations of the molecules in the excited state, which are responsible for the fluorescence quenching.[49] To confirm this assumption, fluorescence spectra were recorded in a solvent of higher viscosity. Thus, with an increasing content of glycerol, the fluorescence quantum yield of **2*m*** increased (50 wt% glycerol Φ_{fl} = 0.06, 80 wt% Φ_{fl} = 0.18, 100 wt% Φ_{fl} = 0.46). The viscosity had a weaker impact on the fluorescence quantum yield of **2*p*** (100 wt% glycerol Φ_{fl} = 0.075) and showed no effect at all for the *ortho* isomer **2*o***.

Quenching by DNA can be attributed to intermolecular charge or electron transfer between the excited ligand and the DNA base pairs.[56] Both *ortho* and *para* isomers participate in such processes, which strongly supersede the enhancement effect of restricted conformational changes. Again, we address the role of the nucleotide bases AT versus GC next.

10.1002/chem.202101918

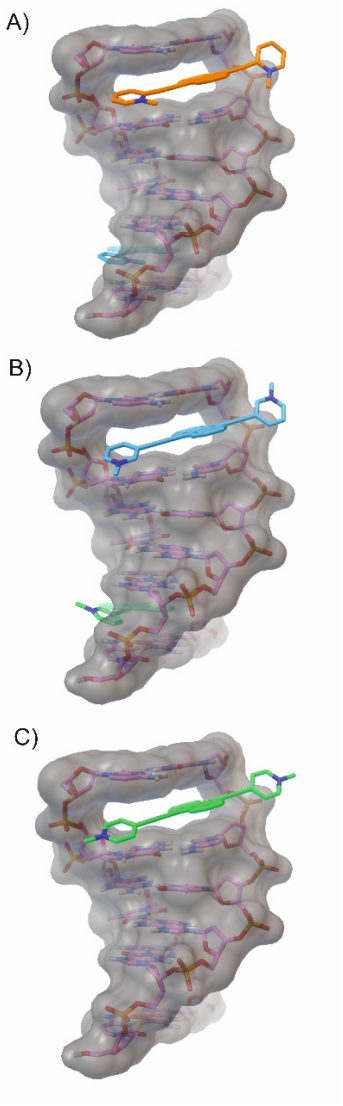

Figure 9. Optimized docking geometries of pyridinium alkynylanthracenes in a $(CGATCG)_2$ hexamer A) **2o**, B) ***2m*** and C) ***2p***.

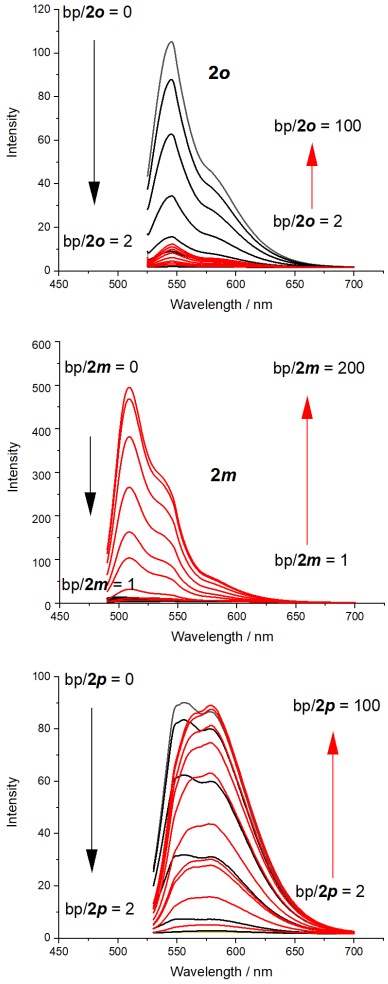

Figure 10. Fluorimetric titrations of pyridinium alkynylanthracenes **2o**–***p*** with ct-DNA.

Fluorimetric titrations with poly(dA:dT) showed, in analogy to ct-DNA, quenching of the fluorescence of **2o**, increasing fluorescence of non-fluorescent ***2m*** and no changes for ***2p***, whereas quantitative quenching of the emission was observed for all three isomers on titration with poly(dG:dC). The latter quenching could be caused by an electron transfer from the guanine residues to the excited sensitizer. According to literature data,[57] poly(dG:dC) is oxidized at potentials >1.3 V, which is below the potentials of 1.71 V for **2o** and 1.55 V for ***2p*** and therefore in agreement with fluorescence quenching. Poly(dA:dT) is oxidized at a higher potential of ~1.7 V and causes quenching only for **2o** but not for ***2p.*** These findings show that DNA interaction causes severe implications for exited state processes of the three isomers, as a result of the conjugation. Based on the fluorimetric titrations, intrinsic binding constants K_B were determined by a modified Scatchard analysis (Table 1, Figure S10, Supporting Information).[58]

Table 1. Binding constants (K_B) and fraction of base pairs, which bind to the ligand, *n*, of pyridinium alkynylanthracenes **2o**–***p*** with ct-DNA, poly(dA:dT) and poly(dG:dC).

	ct-DNA		poly(dA:dT)		poly(dG:dC)	
	K_B / M^{-1}	*n*	K_B / M^{-1}	*n*	K_B / M^{-1}	*n*
2o	-	-	1.69 x 10^{7}[a]	0.55	2.05 x 10^{6}[b]	0.48
2m	1.10 x 10^{6} [a]	0.54	-	-	3.71 x 10^{6}[b]	0.58
2p	-	-	-	-	5.28 x 10^{7}[b]	0.64

[a] Determined from photometric titration data by the method of McGhee/Hippel (see Figure S11 and S12, Supporting Information); [b] Determined by Scatchard analysis from fluorimetric titration data (Figure S10, Supporting Information).

The binding constants with poly(dG:dC) between 0.2–5 x 10^{7} M^{-1} are relatively high as compared to literature known anthracenes with alkyl ammonium substituents (ranging between 2–3 x 10^{6} M^{-1}).[46] All three isomers exhibit binding densities of ~ 2 base pairs per dye, which points at an intercalative association with neighbor exclusion.[47,59] Isomer ***2p*** exhibited a stronger affinity towards poly(dA:dT), which could also be confirmed by sequential titration of ***2p***, starting with poly(dG:dC) causing

fluorescence quenching followed by titration with poly(dA:dT) that resulted in an increase of fluorescence instead (Figure S13, Supporting Information), thus, indicating a redistribution of the ligand from the poly(dG:dC) to poly(dA:dT).

Fluorimetric titrations have therefore shown that pyridinium anthacenes indeed interact in their excited states with DNA, which holds in particular for the *ortho* derivative **2*o***. In the final section, we address the implication of this feature on photochemical processes.

Photochemical properties of the pyridinium alkynylanthracenes in the presence of DNA.

Irradiation of a mixture of the pyridinium alkynylanthracenes **2*o*–*p*** bound to ct-DNA (excess 8 bp/ligand) in the presence of **GLYANT** as singlet-oxygen trapping reagent resulted in no conversion of the latter to **GLYANTO2**. However, when the ligands were bound to poly(dA:dT) (2 bp/ligand) instead, a significant enhancement of the photosensitizing activity of **2*o*–*p*** was observed as the trapping reagent was transformed significantly faster. It has to be noted that the trapping reagent showed no tendency to interact with DNA as confirmed by the above-mentioned DNA melting and absorbance experiments (see Figures S15 and S16 Supporting Information). From the determination of pseudo-first order rates of disappearance of **GLYANT** normalized to the rate of **GLYANT** with **2*m***, reactivities of the three isomers in poly(dA:dT) and poly(dG:dC) could be compared (Figure 11a–c, Figures S17–S21, Supporting Information).

By interaction with poly(dA:dT), the rate constants of the reaction of the trapping reagent are enhanced by a factor of ~ 5 relative to the rate constants of the unbound species. Comparison between the rates of the three isomers revealed the fastest reaction of **2*p***/p(dA:dT) (50 times faster than **2*m*** alone). In order to unequivocally assign the conversion of the trapping reagent to a Type II reaction mechanism involving $^1O_2$, we performed additional irradiation experiments with sensitizer **2*m*** (Figure 12). Firstly, irradiation with poly(dA:dT) was repeated under anaerobic conditions. This caused the conversion of **GLYANT** to slow down by a factor >15, which proves that oxygen is involved. In the second control experiment, H_2O was exchanged with D_2O, in which the reaction proceeded faster because of the longer lifetime of $^1O_2$ in this medium. With poly(dA:dT) the reaction rate was enhanced more than tenfold relative to that in H_2O, pointing at the involvement of $^1O_2$. In the third experiment, irradiation was performed in the presence of the $^1O_2$ quencher sodium azide (1 mM), which showed no effect on quenching the excited state fluorescence of **2*m***.[60] In this case, the reactivity was reduced by a factor of ~13 as compared to the reaction of the trapping reagent without quencher, confirming a Type II reaction as major reaction pathway. Thus, the photochemical processes following excitation of **2*o*–*p***, are switched by poly(dA:dT) from an ET to a $^1O_2$ reaction.

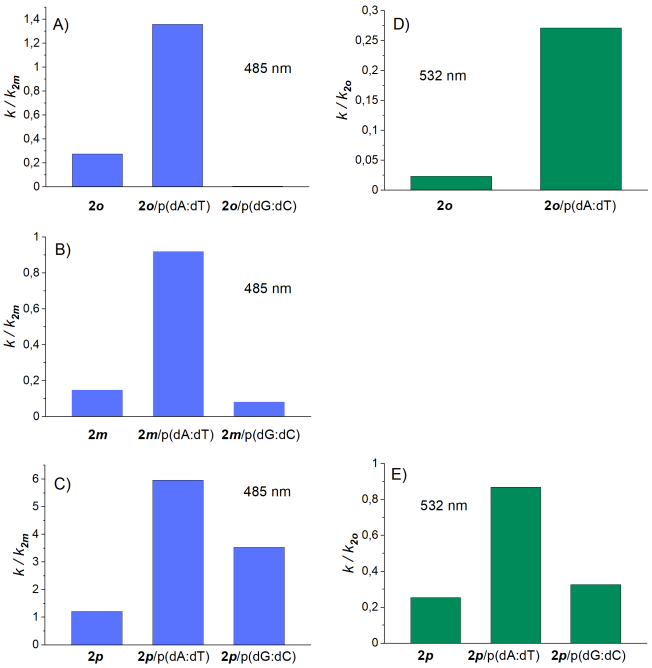

Figure 11. Photosensitized $^1O_2$ generation on irradiation of the pyridinium alkynylanthracenes **2*o*–*p*** determined by the photooxygenation of **GLYANT** alone, in the presence of 2 eq of poly(dA:dT) and 2 bp of poly(dG:C). All values are referenced to the reaction rate of **2*m*** as standard in water with no DNA. The green bars indicate irradiation at 532 nm (**2*p*** as standard), the blue bars irradiation at 485 nm.

With poly(dG:dC) only **2*p*** showed an enhancement of reactivity, while this polynucleotide caused reduced reactivity for the other two isomers. Thus, with poly(dG:dC) **GLYANT** was converted ~ 3 times faster as compared with the reaction without the polynucleotide. As shown in the beginning, the unbound photosensitizers turned out to be unstable upon irradiation, as **2*m*** and **2*p*** bleached rapidly in free form. Notably, the association to DNA also had an effect on the photostability because **2*p*** showed no tendency to bleach (Figure 13). Also, **2*m*** persisted longer in the presence of the two polynucleotides (compare Figure 3c and 13c). Only **2*o*** showed different behavior, while it is stable in its free form and when bound to poly(dG:dC), it showed also slight decomposition in poly(dA:dT).

The experiments carried out under anaerobic conditions and with the quencher sodium azide revealed that DNA interaction has almost quantitatively switched off the photoinduced ET reaction between **2*p*** or **2*m*** and the trapping reagent. This may be ascribed to a shielding effect, keeping the potential ET donor **GLYANT** apart from the electron accepting sensitizer. However, the main merit provided by DNA interaction is the mitigation of the inadvertent intramolecular ET process causing decomposition of the excited sensitizer. This mechanistical change can be rationalized by the hydrophobicity of the polynucleotide environment preventing separation of charges arising from intramolecular ET and the reduced accessibility of water molecules responsible for consecutive reaction steps.

10.1002/chem.202101918

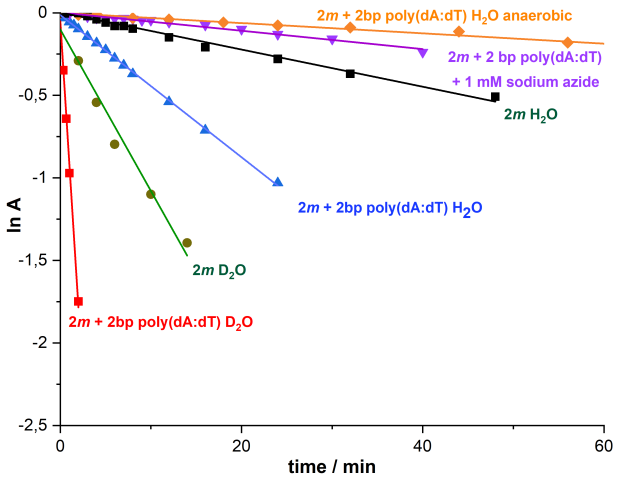

Figure 12. Decay of the trapping reagent **GLYANT** *vs* time upon irradiation of the pyridinium alkynylanthracene ***2m***. The black curve shows the decay by irradiation of ***2m*** at 485 nm in H_2O and the green curve the same reaction in D_2O. The blue and red curves show the decays in the presence of poly(dA:dT) for H_2O and D_2O, respectively. Violet: Decay with poly(dA:dT) in the presence of sodium azide (1 mM); orange: decay with poly(dA:dT) in the absence of oxygen.

This advantage of a change from an ET process toward a $^1O_2$ reaction is more pronounced with poly(dA:dT), whereas poly(dG:dC) can also impede production of $^1O_2$ as seen for ***2o***. In this case a possible channel of deactivation of the S_1 state is the ET from the reducing guanine residues. Notably, only the *para* derivative ***2p*** shows also enhanced $^1O_2$ production with both types of nucleotides. Yet, ***2p*** is not a strong oxidant such as ***2o*** to react with GC but still strong enough to prevent self-decomposition in contrast to ***2m***.

It is worth mentioning that the strong bathochromic shifts of the absorption bands of the three pyridinium alkynylanthracenes ***2o*** and ***2p*** imposed by all nucleotides allowed to excite the DNA-bound forms with green light, which is not absorbed by the unbound form (see Figure 11d, 11e and Figure S22, Supporting Information). We derived singlet oxygen quantum yields Φ_Δ at 532 nm irradiation with tetrakis(4-sulfonatophenyl) porphyrin TPPS as reference (Table 2, Figure S23, Supporting Information). In addition, we determined the ratio between the reaction of the trapping reagent and the decomposition of the sensitizing dye. A high value indicates a good resilience of the sensitizer; small values show that the sensitizer undergoes preferentially an irreversible Type I reaction. Thus, ***2o*** produces 10 times more $^1O_2$ when bound to poly(dA:dT) as compared with its free form. This is a crucial feature for PDT applications, because excitation of the dye should exclusively occur in the vicinity of DNA.

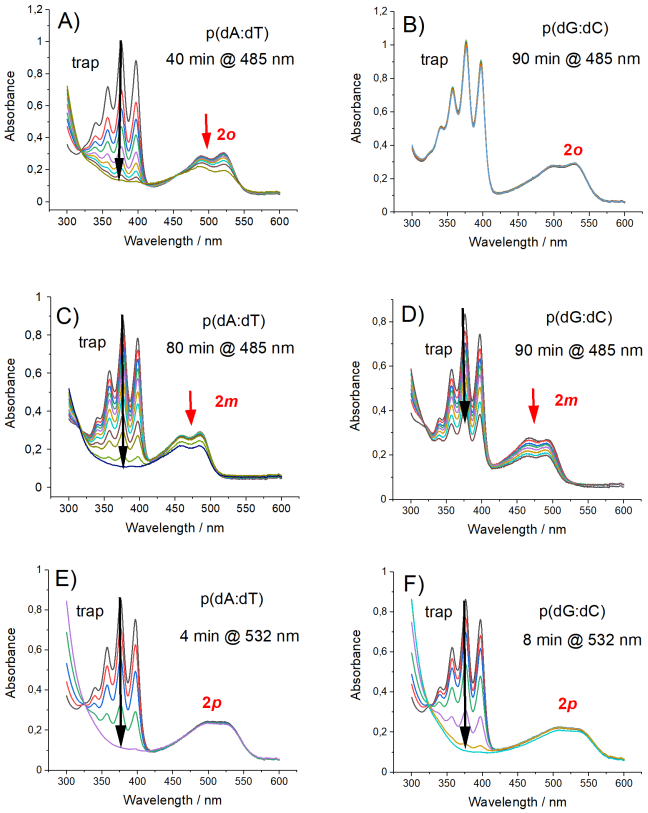

Figure 13. Reactions of the trapping reagent **GLYANT** and the sensitizers ***2o–p*** caused by irradiation in the presence of poly(dA:dT) and poly(dG:dC).

Table 2: Singlet oxygen quantum yields from rate constants and bleaching index as ratio $k_{trapping\ reagent}/k_2$ of pyridinium alkynylanthracenes ***2o–p.***

acene	Φ_Δ[a] (free)	$k_{trapping\ reagent}/k_2$ (free)	Φ_Δ (AT-bound)	$k_{trapping\ reagent}/k_2$ (AT-bound)
2p	0.07	1.8	0.22	38
2o	0.01	>100	0.10	12

[a] Excitation at 532 nm; standard TPPS Φ_Δ=0.64[61]

Conclusion

The three isomeric pyridinium alkynylanthracenes ***2o–p*** show a binding affinity toward ct-DNA, poly(dA:dT) and poly(dG:dC), as confirmed by the increased T_m values and the appearance of a red shift and a vibronic fine structure in the UV/vis spectra. On the basis of the negative signs of the LD spectra with ct-DNA and negative ICD effects of transitions, whose calculated dipole moments are oriented parallel to the molecular short axis, we propose an intercalative binding mode of the three anthracene isomers with the alkynyl pyridyl axis oriented parallel to the long axis of the base pairs of the nucleotide.

For the investigation of their photochemical features, we synthesized the new trapping reagent **GLYANT**. In the absence of DNA, irradiation of ***2o–p*** with light fitting to their long wavelength absorbance maxima caused a consumption of the

trapping reagent and the photosensitizers, except for the *ortho* derivative **2*o***. Several control experiments under anaerobic conditions and use of deuterated solvents confirm two reaction pathways, one involving $^1O_2$, the other electron transfer from the trapping reagent to the excited pyridinium anthracene. By use of cyclic voltammetry and UV/vis spectroscopy, the excited state reduction potentials of the three sensitizers were determined. These data reveal that **2*o*** and **2*p*** act as strong oxidants in their excited states, which leads to an ET processes. Also, the inherent anthracene units of the pyridinium alkynylanthracenes undergo ET. Because of these ET processes, the three compounds are unsuitable as sensitizers for the generation of $^1O_2$ in their free forms.

In contrast, the ability to generate $^1O_2$ is switched on for all three derivatives in the presence of poly(dA:dT), as clearly indicated by the increased oxidation of **GLYANT**. The prevalence of the $^1O_2$ pathway over the ET path is confirmed by the lack of reactivity under anaerobic conditions and the strong reactivity enhancement in deuterated solvents. The main advantage gained from this interaction is that the sensitizers are stabilized and their self-decomposition is suppressed. This effect is caused by the hydrophobic environment provided within the intercalation pocket. However, for the *ortho* isomer **2*o*** with the highest oxidation potential in its excited state, ET from adenine bases can also occur causing a quenching of fluorescence and self-decomposition of the sensitizer. The *para* isomer **2*p***, where the reaction of the trapping reagent exhibits the highest reactivity, is the only example, where a switching is also achieved by polynucleotides carrying guanine. It is therefore persistent against self-decomposition but does not provide sufficient oxidation power to oxidize the polynucleotide bases. Future studies will focus on the application of these new pyridinium alkynylanthracenes to selectively damage DNA in vitro and in vivo.

Experimental Section

Detailed information about the materials used, all spectroscopic techniques, DNA melting studies, determination of binding constants, irradiation experiments, calculations and molecular modelling is given in in the Supporting Information.

Synthesis of *bis*-9,10-(pyridylalkynyl)anthracenes 5*o*—*p* by Sonogashira coupling. Anthracenes **5*o*—*p*** were prepared according to an established procedure, affording yields of >80%.[37] Dibromoanthracene (**4**) (336 mg, 1 mmol), $[Pd(PPh_3)_2Cl_2]$ (60 mg, 0.08 mmol) and CuI (100 mg, 0.52 mmol) were placed in a round bottom flask and dissolved in dry THF (8 mL) and dry *i*Pr_2NH (8 mL). After degassing by three freeze-pump-thaw cycles, the flask was filled with argon and sealed with a septum. At 80 °C the literature known pyridyl acetylenes (2.1 mmol) (**3*o*—*p***)[64] were added in neat *via* syringe pump over a period of 4.5 h. Thereafter, the solvent was evaporated and the residue was suspended in methanol. The precipitate was filtered and the residue was dissolved in hot $CHCl_3$. After hot filtration, the product precipitated upon cooling.

***Bis*-9,10-(2-pyridylethynyl)anthracene 5*o*:** Yield 315 mg (84%), yellow crystals. Mp. > 300 °C (Decomposition). ^{1}H NMR (400 MHz, $CDCl_3$): δ=7.35 (2H, *J*=4.2 Hz, 13.6 Hz, 4-HPy), 7.69 (4H, dd, *J*=3.45 Hz, 9.89 Hz, H-1, H-4, H-5, H-8), 7.81 (4H, 2d, *J*=3.65 Hz, 9.89 Hz, 3-HPy, 5-HPy), 8.76-8.78 (6H, m, 2-H, 3-H, 6-H, 7-H, 6-HPy). ^{13}C NMR (80 MHz, $CDCl_3$): δ= 86.1 (s, AlkynylANT), 101.6 (s, AlkynylPy), 118.2 (C9, C10), 123.0 (s, C11, C12, C13, C14, C15), 127.2 (d, C1, C2, C3, C4, C5, C6, C7, C8), 127.6 (d, CPy4), 132.4 (d, CPy3), 136.3 (d, CPy5), 143.5 (s,CPy2), 150.4 (d, CPy6); IR (cm^{-1}, ATR) $\tilde{\nu}$=3666 (m), 2982 (s), 2903 (s), 2199 (m), 1575 (m), 1558 (m), 1462 (m), 1425 (m), 1249 (m), 1048 (s), 755 s); HRMS (ES+): m/z: calcd for $C_{28}H_{16}N_2$: 382.1470 [M]; found 382.1464 [M].

***Bis*-9,10-(3-pyridylethynyl)anthracene 5*m*:** Yield 319 mg (87%), yellow crystals. Mp. 270-273 °C. ^{1}H NMR (400 MHz, $CDCl_3$): δ=7.42 (2H, dd, *J*=3.4Hz, 7.85 Hz, 3-HPy), 7.70 (4H, *J*=3.4 Hz, 9.9 Hz, H-1, H-4, H-5, H-8), 8.07 (2H, d, *J*=7.9 Hz, 4-HPy), 8.67-8.69 (6H, H-2, H-3, H-6, H-7, 6-HPy), 9.04 (2H, s 2-HPy). ^{13}C NMR (80 MHz, $CDCl_3$): δ=89.5 (AlkynylANT), 98.9 (s, AlkynylPy), 118.2 (s, C9, C10), 120.5 (s, CPy3), 123.2 (s, C11, C12, C13, C14, C15), 127.1 (d, C2, C3, C6, C7), 127.2 (d, C1, C4, C5, C8), 132.1 (CPy4), 138.4 (CPy5), 149.0 (CPy2), 152.2 (d, CPy6); IR (cm^{-1}, ATR) $\tilde{\nu}$=3667 (m), 2979 (s), 2903 (s), 2196 (m), 1901 (w), 1715 (w), 1476 (m), 1404 (m), 1232 (m), 1184 (m), 1017 (m); HRMS (ES+): m/z: calcd for $C_{28}H_{16}N_2$: 382.1470 [M]; found 382.1447 [M].

***Bis*-9,10-(4-pyridylethynyl)anthracene 5*p*:** Yield 321 mg (89%), yellow crystals. Mp. 283-286 °C. ^{1}H NMR (400 MHz, CDCl3): δ=7.65 (4H, d, *J*=5.6 Hz, 3-HPy, 5-HPy), 7.72 (4H, dd, *J*=3.4Hz, 9.9 Hz, H-2, H-3, H-6, H-7), 8.67 (dd, *J*=9,9 Hz, 3.4 Hz, H-1, H-4, H-5, H-8), 8.75 (4H, d, *J*=5.6 Hz, 2-HPy, 6-HPy). ^{13}C NMR (80 MHz, $CDCl_3$): δ=90.6 (AlkynylANT), 99.7 (s, AlkynylPy), 118.2 (s, C9, C10), 125.4 (s, C11, C12, C13, C14, C15), 127.0 (d, C2, C3, C6, C7), 127.4 (d, C1, C4, C5, C8), 131,2 (s, CPy4), 132.2 (d, CPy3, CPy5), 150.0 (d, CPy2, CPy6); IR (cm^{-1}, ATR) $\tilde{\nu}$=3667 (m), 2979 (s), 2902 (s), 2200 (m), 1587 (m), 1403 (m), 1213 (m), 1062 (s); HRMS (ES+): m/z: calcd for $C_{28}H_{16}N_2$: 382.1470 [M]; found 382.1437 [M].

Synthesis of the methyl 9,10-(pyridiniumalkynyl)anthracenes 2*o*—*p*. The pyridylalkynyl anthracenes **5*o*—*p*** (0.5 mmol) were methylated by heating in DMF in the presence of 3 eq of dimethyl sulfate at 100 °C for 24 h. After removal of DMF at reduced pressure, the methyl 9,10-(pyridiniumalkynyl)anthracenes **2*o*—*p*** were recrystallized in methanol.

9,10-Bis(2-methylpyridinium-1-yl-ethynyl)anthracene sulfate 2*o*: Yield 290 mg (96 %), orange solid. Mp. > 300 °C (Decomposition). ^{1}H NMR (400 MHz, DMSO-d_6): δ=4.70 (6H, CH_3), 7.97 (4H, dd, *J*=2.8 Hz, 6.4 Hz, H-1, H-4, H-5, H-8), 8.22 (2H, m, 4-HPy), 8.75 (6H, m, 2-H, 3-H, 6-H, 7-H, 5-HPy), 8.85 (2H, d, *J*=7.8 Hz, 3-HPy), 9.28 (2H, d, *J*=5.9 Hz, 6-HPy). ^{13}C NMR (80 MHz, DMSO-d_6): δ=48.3 (s, CH_3), 94.0 (s, AlkynylANT), 100.9 (s, AlkynylPy), 117.5 (s, C9, C10), 127.2 (d, CPy4), 127.8 (s, C11, C12, C13, C14, C15), 130.0 (d, C2, C3, C6, C7), 132.4 (d, C1, C4, C5, C8), 132.8 (d, CPy3), 137.2 (s, CPy2), 145.3 (d, CPy5), 147.9 (d, CPy6); IR (cm^{-1}, ATR) $\tilde{\nu}$=3063 (w), 3032 (w), 2196 (m), 1628 (m), 1506 (m), 1452 (m), 1229 (s), 1165 (s), 1032 (s), 839 (s), 761 (s); HRMS (ES+): m/z: calcd for $C_{30}H_{22}N_2$: 410.1782 [M]; found 205.0887 [M^{2+}].

9,10-Bis(3-methylpyridinium-1-yl-ethynyl)anthracene sulfate 2*m*: Yield 285 mg (92 %), orange solid. Mp. > 300°C (Decomposition). ^{1}H NMR (400 MHz, DMSO-d_6): δ=4.45 (6H, CH_3), 7.91 (4H, *J*=3.4 Hz, 9.7 Hz, H-1, H-4, H-5, H-8), 8.30 (2H, dd, *J*=6.1 Hz, 7.7 Hz, 5-HPy), 8.83 (4H, dd, *J*=3.4 Hz, 9.7 Hz, 2-H, 3-H, 6-H, 7-H), 9.09 (2H, d, *J*=6.1 Hz, 4-HPy), 9.12 (2H, d, *J*=8.2 Hz, 6-HPy), 9.75 (2H, s, 2-HPy). ^{13}C NMR (80 MHz, DMSO-d_6): δ=48.7 (s, CH_3), 92.3 (s, AlkynylANT), 96.5 (s, AlkynylPy), 117.1 (s, C9, C10), 122.9 (s, C11, C12, C13, C14, C15), 127.3 (d, CPy5), 128.1 (d, CPy4), 129.1 (d, C2, C3, C6, C7), 132.1 (d, C1, C4, C5, C8), 147.1 (d, CPy2), 145.6 (s, CPy3), 148.6 (d, CPy6); IR (cm^{-1}, ATR) $\tilde{\nu}$=3667 (w), 2979 (s), 2902 (s), 2198 (m), 1505 (m), 1452 (m), 1230 (s), 1170 (m), 1034 (s), 840 (m); HRMS (ES+): m/z: calcd for $C_{30}H_{22}N_2$: 410.1782 [M]; found 205.0894 [M^{2+}].

9,10-Bis(4-methylpyridinium-1-yl-ethynyl)anthracene sulfate 2*p*: Yield 292 mg (94 %), orange solid. Mp. > 300 °C (Decomposition). ^{1}H NMR (400 MHz, DMSO-d_6): δ=4.39 (6H, CH_3), 7.94 (4H, dd, *J*=3.4 Hz, 9.8 Hz, H-1, H-4, H-5, H-8), 8.67 (4H, d, *J*=9.1 Hz, 3-HPy, 5-HPy), 8.85 (4H, dd, *J*=3.4 Hz, 9.8 Hz), 2-H, 3-H, 6-H, 7-H), 9.15 (4H, d, *J*=9.1 Hz, 2-HPy, 6-HPy). ^{13}C NMR (80 MHz, DMSO-d_6): δ=48.3 (CH_3), 97.6 (s, AlkynylANT), 99.3 (s, AlkynylPy), 118.1 (s, C9, C10), 127.4 (d, C2, C3, C6, C7), 129.5 (d, C1, C4, C5, C8), 129.7 (s, C11, C12, C13, C14, C15), 132.5 (CPy2, CPy4), 138.1 (CPy1), 146.1 (CPy3, CPy5); IR (cm^{-1}, ATR) $\tilde{\nu}$=3064 (w),

3032 (w), 2198 (m), 1628 (m), 1505 (m), 1452 (m), 1230 (s), 1169 (s), 1031 (s), 840 (s), 763 (s); HRMS (ES+): m/z: calcd for $C_{30}H_{22}N_2$: 410.1782 [M]; found 205.0892 [M^{2+}].

Synthesis of GLYANT. The trapping reagent **GLYANT** was synthesized from anthraquinone (**6**),[38] which was reduced with $NaBH_4$ to give anthrahydroquinone (**7**) followed by addition of the literature known tetra-*O*-acetyl-α-*D*-glucopyranosyltrichloracetimidat (**8**).[39] The acetyl groups of anthracene **9** were finally cleaved to give the free anthracene sugar **GLYANT**.

9,10-Bis-(1-*O*-2,3,4,6-tetra-*O*-acetyl-*β*-D-glucopyranosyl)anthracene (9). Note that the intermediate anthrahydroquinone (**7**) is rapidly oxidized by air and therefore all steps have to carried out under inert gas atmosphere using a Schlenck apparatus. Anthraquinone (**6**) (1.041 g, 5 mmol) was dissolved in diglyme (25 mL) and $NaBH_4$ (0.189 g, 5 mmol) was added. After 1 h the reaction mixture was transferred under argon into argon saturated 1M HCl (1 L). A precipitate formed, which was filtered under argon and washed with argon saturated MeOH (50 mL). The intermediate anthrahydroquinone (**7**) was then dried under vacuum for 6 h. For the coupling reaction **7** was dissolved in dry dichloromethane (100 mL) in a round bottom flask and 2,3,4,6-Tetra-*O*-acetyl-*α*-D-glucopyranosyltrichloracetimidat (**8**, 4.927 g, 10 mmol) was added. The solution mixture was cooled to −15 °C and $BF_3{\cdot}Et_2O$ (0.13 mL, 1 mmol) dissolved in dichloromethane (1 mL) was added within 30 min. The solution was stirred for 16 h at room temperature. The solution was filtered over celite, washed with saturated $NaHCO_3$ solution and water and dried with Na_2SO_4. After the solvent was removed by evaporation, the crude product was purified by column chromatography (PE/EtOAc 1:1). Yield 3.708 g (83 %) white solid. Mp. 209–210 °C (Decomposition); R_f = 0.19 (PE/EtOAc 1:1); $[\alpha]^{25}_D$ = +56°, *c* = 1.00, $CHCl_3$; ^{1}H NMR (600 MHz, $CDCl_3$): δ = 1.80 (2s, 6H; 6-OAc), 2.01 (2s, 6H; 4-OAc), 2.08 (2s, 6H; 3-OAc), 2.23 (2s, 6H; 2-OAc), 3.52 (2ddd, *J* = 9.9, 5.5, 2.7 Hz, 2H; 5-H), 3.89 (2dd, *J* = 12.1, 2.7 Hz, 2H; 6a-H), 4.23 (2dd, *J* = 12.1, 5.6 Hz, 2H; 6b-H), 5.21 (2d, *J* = 8.1 Hz, 2H; 1-H), 5.24 (2dd, *J* = 9.9, 9.4 Hz, 2H; 4-H), 5.33 (2dd, *J* = 9.7, 9.4 Hz, 2H; 3-H), 5.64 (2dd, *J* = 9.7, 8.1 Hz, 2H; 2-H), 7.47–7.50 (m, 4H; 2-ArH, 3-ArH, 6-ArH, 7-ArH), 8.38–8.41 ppm (m, 4H; 1-ArH, 4-ArH, 5-ArH, 8-ArH); ^{13}C NMR (125 MHz, $CDCl_3$): δ = 20.5 (2q; OAc-6), 20.6 (2q; OAc-4), 20.7 (2q; OAc-3), 20.9 (2q; OAc-2), 61.8 (2t; C-6), 68.7 (2d; C-4), 71.9 (2d; C-5), 72.2 (2d; C-2), 73.1 (2d; C-3), 102.8 (2d; C-1), 122.7 (4d; ArC-1, ArC-4, ArC-5, ArC-8), 125.3 (4s; ArC-4a, ArC-8a, ArC-9a, ArC-10a), 125.7 (4d; ArC-2, ArC-3, ArC-6, ArC-7), 144.9 (2s; ArC-9, ArC-10), 169.4 (2s; OAc-2), 169.5 (2s; OAc-4), 170.4 (2s; OAc-6), 170.5 ppm (2s; OAc-3); IR (Film): $\tilde{\nu}$ = 2960 (w), 1746 (s), 1436 (w) 1362 (m), 1212 (s), 1037 (s), 756 cm^{-1} (m); HRMS (ESI-Q-TOF): *m/z* calc. for $C_{42}H_{46}NaO_{20}$ (M + Na^+): 893.2480; found: 893.2521; Elemental analysis (%) for $C_{42}H_{46}O_{20}$ (870.81): C 57.93, H 5.32; found: C 57.60, H 5.32.

9,10-Bis-(1-*O*-*β*-D-glucopyranosyl)anthracene (GLYANT). The acetyl glucopyranosylanthracene **9** (2.612 g, 3 mmol) was dissolved in methanol (30 mL) and a 1M solution of sodium methanolate in methanol (2.4 mL) was added. The mixture was stirred for 16 h after which acidic ion exchanger (1 g) was added followed by filtration. After removal of the solvent **GLYANT** was obtained. Yield 1.602 g (99 %) white solid. Mp. 242–243 °C; R_f = 0.19 (EtOAc/MeOH 4:1); $[\alpha]^{24}_D$ = +96°, *c* = 1.00, MeOH; ^{1}H NMR (500 MHz, CD_3OD): δ = 3.04 (ddd, *J* = 9.4, 4.2, 3.3 Hz, 2H; 5-H), 3.51 (dd, *J* = 9.2, 9.0 Hz, 2H; 3-H), 3.54 (dd; *J* = 9.4, 9.0 Hz, 2H; 4-H), 3.60 (dd, *J* = 11.8, 3.3 Hz, 2H; 6_a-H), 3.62 (dd, *J* = 11.8, 4.2 Hz, 2H; 6_b-H), 3.83 (dd, *J* = 9.2, 7.9 Hz, 2H; 2-H), 5.00 (d, *J* = 7.9 Hz, 2H; 1-H), 7.44–7.48 (m, 4H; 2-H, 3-ArH, 6-ArH, 7-ArH), 8.68–8.71 ppm (m, 4H; 1-ArH, 4-ArH, 5-ArH, 8-ArH); ^{13}C NMR (100 MHz, CD_3OD): δ = 62.6 (t; C-6), 71.5 (d; C-4), 76.0 (d; C-2), 77.9 (d; C-5), 78.2 (d; C-3), 107.3 (d; C-1), 124.6 (d; ArC-1, ArC-4, ArC-5, ArC-8), 126.1 (d; ArC-2, ArC-3, ArC-6, ArC-7), 126.8 (s; ArC-4a, ArC-8a, ArC-9a, ArC-10a), 146.8 ppm (s; ArC-9, ArC-10); IR (Film): $\tilde{\nu}$ = 3339 (br), 2361 (w), 1636 (m), 1353 (w), 1070 (s), 1014 cm^{-1} (s); HRMS (ESI-Q-TOF): *m/z* calculated for $C_{26}H_{30}NaO_{12}$ (M + Na^+): 557.1629; found: 557.1623; Elemental analysis (%) for $C_{26}H_{30}O_{12}$ (534.51): C 58.42, H 5.66; found: C 58.54, H 5.56.

Preparative photooxygenation of GLYANT (10) using the sensitizer methylene blue. GLYANT (534 mg, 1 mmol) was dissolved in MeOH (10 mL) and methylene blue (3 mg, 1 mol%) was added. The solution was irradiated for 1 h by two sodium lamps (1000 W), while oxygen was continuously bubbled through the solution. The solvent was evaporated and the product purified by column chromatography (EtOAc/MeOH 10:1, reversed phase).

9,10-Bis-(1-*O*-*β*-D-glucopyranosyl)-9,10-dihydro-9,10-epidioxidoanthracene (GLYANTO2). Yield 538 mg (99 %) white solid. Mp. 119−121 °C; R_f = 0.23 (EtOAc/MeOH 10:1, reversed phase); $[\alpha]^{23}_D$ = +12°, *c* = 0.99, MeOH; ^{1}H NMR (500 MHz, CD_3OD): δ = 3.29 (ddd, *J* = 9.6, 5.6, 2.1 Hz, 2H; 5-H), 3.42 (dd, *J* = 9.6, 8.9 Hz, 2H; 4-H), 3.46 (dd, *J* = 9.0, 8.9 Hz, 2H; 3-H), 3.56 (dd, *J* = 9.0, 7.8 Hz, 2H; 2-H), 3.70 (dd, *J* = 12.3, 5.6 Hz, 2H; 6_b-H), 3.87 (dd, *J* = 12.3, 2.1 Hz, 2H; 6_a-H), 5.21 (d, *J* = 7.8 Hz, 2H; 1-H), 7.24−7.29 (m, 4H; 2-ArH, 3-ArH, 6-ArH, 7-ArH), 7.92−7.97 ppm (m, 4H; 1-ArH, 4-ArH, 5-ArH, 8-ArH); ^{13}C NMR (100 MHz, CD_3OD): δ = 62.5 (t; C-6), 71.4 (d; C-4), 75.3 (d; C-2), 77.8 (d; C-3), 78.5 (d; C-5), 100.6 (d; C-1), 104.2 (s; ArC-9, ArC-10), 122.1 (d; ArC-4, ArC-5), 122.2 (d; ArC-1, ArC-8), 128.7 (d; ArC-2, ArC-7), 128.9 (d; ArC-3, ArC-6), 139.4 (s; ArC-8a, ArC-9a), 139.6 ppm (s; ArC-4a, ArC-10a); IR (Film): $\tilde{\nu}$ = 3319 (br), 2161 (w), 2.131 (m), 1344 (w), 1098 (s), 1064 (m), 1021 cm^{-1} (s); HRMS (ESI-Q-TOF): *m/z* calculated for $C_{26}H_{30}NaO_{14}$ (M + Na^+): 589.1528; found: 589.1521.

Acknowledgements

We thank Melanie Metz (University of Potsdam) and Jessica Hermann (University of Siegen) for the synthesis of compounds (M. M.) and LD measurements (J. H.).

Keywords: Anthracene • DNA • Intercalations • Photochemistry • Singlet Oxygen

[1] S. Kwiatkowski, B. Knap, D. Przystupski, J. Saczko, E. Kędzierska, K. Knap-Czop, J. Kotlińska, O. Michel, K. Kotowski, J. Kulbacka, *Biomed. Pharmacother.* **2018**, *106*, 1098–1107.

[2] B. Q. Spring, I. Rizvi, N. Xu, T. Hasan, *Photochem. Photobiol. Sci.* **2015**, *14*, 1476–1491.

[3] L. Benov, *Med. Princ. Pract.* **2015**, *24*, 14–28.

[4] D. E. J. G. J. Dolmans, F. D, R. K. Jain, *Nat. Rev. Cancer* **2003**, *3*, 375–380.

[5] J. M. Dąbrowski, L. G. Arnaut, *Photochem. Photobiol. Sci.* **2015**, *14*, 1765–1780.

[6] P. Agostinis, K. Berg, K. A. Cengel, T. H. Foster, A. W. Girotti, S. Gollnick, M. Hamblin, A. Juzeniene, D. Kessel, M. Korbelik, J. Moan, P. Mroz, D. Nowis, J. Piette, B. C. Wilson, J. Golab, *CA. Cancer J. Clin.* **2011**, *61*, 250–281.

[7] M. S. Baptista, J. Cadet, P. Di Mascio, A. A. Ghogare, A. Greer, M. R. Hamblin, C. Lorente, S. C. Nunez, M. S. Ribeiro, A. H. Thomas, M. Vignoni, T. M. Yoshimura, *Photochem. Photobiol.* **2017**, *93*, 912–919.

[8] Z. Zhou, J. Song, L. Nie, X. Chen, *Chem. Soc. Rev.* **2016**, *45*, 6597–6626.

[9] F. Vatansever, W. C. M. A. de Melo, P. Avci, D. Vecchio, M. Sadasivam, A. Gupta, R. Chandran, M. Karimi, N. A. Parizotto, R. Yin, G. P. Tegos, M. R. Hamblin, *FEMS Microbiol. Rev.* **2013**, *37*, 955–989.

[10] F. Heinemann, J. Karges, G. Gasser, *Acc. Chem. Res.* **2017**, *50*, 2727–2736.

[11] S. L. H. Higgins, K. J. Brewer, *Angew. Chemie - Int. Ed.* **2012**, *51*, 11420–11422; *Angew. Chem.* **2012,** *124*, 11584-11586.

[12] L. Z. Zhang, G. Q. Tang, *J. Photochem. Photobiol. B Biol.* **2004**, *74*, 119–125.

[13] J. Cadet, T. Douki, J. L. Ravanat, *Acc. Chem. Res.* **2008**, *41*, 1075–1083.

[14] E. Cló, J. W. Snyder, N. V. Voigt, P. R. Ogilby, K. V. Gothelf, *J. Am. Chem. Soc.* **2006**, *128*, 4200–4201.

[15] K. Hirakawa, Y. Nishimura, T. Arai, S. Okazaki, *J. Phys. Chem. B* **2013**, *117*, 13490–13496.

[16] K. Hirakawa, T. Hirano, Y. Nishimura, T. Arai, Y. Nosaka, *J. Phys. Chem. B* **2012**, *116*, 3037–3044.

[17] K. Hirakawa, T. Hirano, *Photochem. Photobiol.* **2008**, *84*, 202–208.

[18] M. R. Deity, P. B. Merkel, *J. Am. Chem. Soc.* **1990**, *112*, 3845–3855.

[19] M. K. Kuimova, G. Yahioglu, P. R. Ogilby, *J. Am. Chem. Soc.* **2009**, *131*, 332–340.

[20] E. Skovsen, J. W. Snyder, J. D. C. Lambert, P. R. Ogilby, *J. Phys. Chem. B* **2005**, *109*, 8570–8573.

[21] N. N. Kruk, B. M. Dzhagarov, V. A. Galievsky, V. S. Chirvony, P. Turpin, *J. Photochem. Photobiol. B Biol.* **1998**, *42*, 181–190.

[22] V. S. Chirvony, V. A. Galievsky, N. N. Kruk, B. M. Dzhagarov, P. Y. Turpin, *J. Photochem. Photobiol. B Biol.* **1997**, *40*, 154–162.

[23] J. J. Nogueira, M. Oppel, L. González, *Angew. Chem. Int. Ed.* **2015**, *54*, 4375–4378; *Angew. Chem.* **2015**, *127*, 4450–4453.

[24] A. Rahman, P. O'Sullivan, I. Rozas, *Medchemcomm* **2019**, *10*, 26–40.

[25] S. Bhaduri, N. Ranjan, D. P. Arya, *Beilstein J. Org. Chem.* **2018**, *14*, 1051–1086.

[26] S. Boga, D. Bouzada, D. García Peña, M. Vázquez López, M. E. Vázquez, *European J. Org. Chem.* **2018**, *2018*, 249–261.

[27] M. Wang, Y. Yu, C. Liang, A. Lu, G. Zhang, *Int. J. Mol. Sci.* **2016**, *17*, 1–24.

[28] A. Rescifina, C. Zagni, M. G. Varrica, V. Pistarà, A. Corsaro, *Eur. J. Med. Chem.* **2014**, *74*, 95–115.

[29] S. Banerjee, E. B. Veale, C. M. Phelan, S. A. Murphy, G. M. Tocci, L. J. Gillespie, D. O. Frimannsson, J. M. Kelly, T. Gunnlaugsson, *Chem. Soc. Rev.* **2013**, *42*, 1601–1618.

[30] W. Xiaoyong, G. Zijian, *Chem. Soc. Rev.* **2013**, *42*, 202–224.

[31] A. C. Komor, J. K. Barton, *Chem. Commun.* **2013**, *49*, 3617–3630.

[32] W. Fudickar, T. Linker, *J. Am. Chem. Soc.* **2012**, *134*, 15071–15082.

[33] W. Fudickar, T. Linker, *J. Org. Chem.* **2017**, *82*, 9285–9262.

[34] W. Fudickar, T. Linker, *Angew. Chem. Int. Ed.* **2018**, *57*, 12971–12975; *Angew. Chem.* **2018**, *130*, 13153–13157.

[35] W. Fudickar, T. Linker, *Bioorg. Med. Chem.* **2020**, *28*, 115432.

[36] S. Winter, E. Weber, L. Eriksson, I. Csöregh, *New J. Chem.* **2006**, *30*, 1808–1819.

[37] B. T. Holmes, W. T. Pennington, T. W. Hanks, *Synth. Commun.* **2003**, *33*, 2447–2461.

[38] M. Bauch, W. Fudickar, T. Linker, *Molecules* **2021**, *26*, 804.

[39] R. R. Schmidt, J. Michel, *Angew. Chem. Int. Ed.* **1980**, *19*, 731–732; *Angew. Chem.* **1980**, *92*, 763–764.

[40] F. Wilkinson, W. P. Helman, A. B. Ross, *J. Phys. Chem. Ref. Data* **1995**, *24*, 663–1021.

[41] D. Rehm, A. Weller, *Isr. J. Chem.* **1970**, *8*, 259–271.

[42] H. Knibbe, D. Rehm, A. Weller, *Berichte der Bunsengesellschaft* **1969**, *73*, 839–845.

[43] X. M. Zhang, F. G. Bordwell, J. E. Bares, J. P. Cheng, B. C. Petrie, *J. Org. Chem.* **1993**, *58*, 3051–3059.

[44] M. A. Liebert, J. Mergny, L. Lacroix, *Oligonucleotides* **2003**, *537*, 515–537.

[45] N. K. Modukuru, K. J. Snow, B. S. Perrin, A. Bhambhani, M. Duff, C. V. Kumar, *J. Photochem. Photobiol. A Chem.* **2006**, *177*, 43–54.

[46] W. B. Tan, A. Bhambhani, M. R. Duff, A. Rodger, C. V. Kumar, *Photochem. Photobiol.* **2005**, *82*, 20.

[47] H. Ihmels, D. Otto, F. Dall'Acqua, A. Faccio, S. Moro, G. Viola, *J. Org. Chem.* **2006**, *71*, 8401–8411.

[48] J. H. Mondal, B. Pramanik, M. N. Shinde, R. Khurana, N. Barooah, A. C. Bhasikuttan, D. Das, J. Mohanty, *J. Phys. Chem. C* **2018**, *122*, 18061–18069.

[49] D. W. Wilson, F. A. Tanious, M. Fernandez-Saiz, C. Ted Rigl, in *Drug-DNA Interact. Protoc.* (Ed.: K.R. Fox), Humana Press, Totowa, NJ, **1997**, pp. 219–240.

[50] B. Norden, M. Kubista, T. Kurucsev, *Q. Rev. Biophys.* **1992**, *25*, 51–170.

[51] S. Basili, A. Bergen, F. Dall'Acqua, A. Faccio, A. Granzhan, H. Ihmels, S. Moro, G. Viola, *Biochemistry* **2007**, *46*, 12721–12736.

[52] M. Kubista, B. Åkerman, B. Nordén, *J. Phys. Chem.* **1988**, *92*, 2352–2356.

[53] C. V. Kumar, E. H. A. Punzalan, W. B. Tan, *Tetrahedron* **2000**, *56*, 7027–7040.

[54] N. K. Modukuru, K. J. Snow, B. S. Perrin, J. Thota, C. V Kumar, *J. Phys. Chem. B.* **2005**, 11810–11818.

[55] O. Trott, A. J. Olson, *J. Comput. Chem.* **2010**, *31*, 455–461.

[56] J. Joseph, E. Kuruvilla, A. T. Achuthan, D. Ramaiah, G. B. Schuster, *Bioconjug. Chem.* **2004**, *15*, 1230–1235.

[57] Y. Paukku, G. Hill, *J. Phys. Chem. A* **2011**, *115*, 4804–4810.

[58] E. F. Healy, *J. Chem. Educ.* **2007**, *84*, 1304.

[59] W. D. Wilson, F. A. Tanious, D. Ding, A. Kumar, D. W. Boykin, P. Colson, C. Houssier, C. Bailly, *J. Am. Chem. Soc.* **1998**, *120*, 10310–10321.

[60] M. Y. Li, C. S. Cline, E. B. Koker, H. H. Carmichael, C. F. Chignell, P. Bilski, *Photochem. Photobiol.* **2001**, *74*, 760.

[61] J. Davila, A. Harriman, *Photochem. Photobiol.* **1990**, *51*, 9–19.

[62] T. M. Fasina, J. C. Collings, D. P. Lydon, D. Albesa-jove, A. S. Batsanov, J. A. K. Howard, P. Nguyen, M. Bruce, A. J. Scott, W. Clegg, S. W. Watt, C. Viney, T. B. Marder, *J. Mater. Chem.* **2004**, *14*, 2395–2404.

[63] M. Surin, P. Samorì, A. Jouaiti, N. Kyritsakas, M. W. Hosseini, *Angew. Chem. Int. Ed.* **2007**, *46*, 245–249; *Angew. Chem.* **2007**, *119,* 249–253.

[64] R. Siddaraj, R. Ningegowda, N. S. Shivananju, B. S. Priya, *Eur. J. Chem.* **2018**, *4*, 317–321.

10.1002/chem.202101918

WILEY-VCH

FULL PAPER

Entry for the Table of Contents

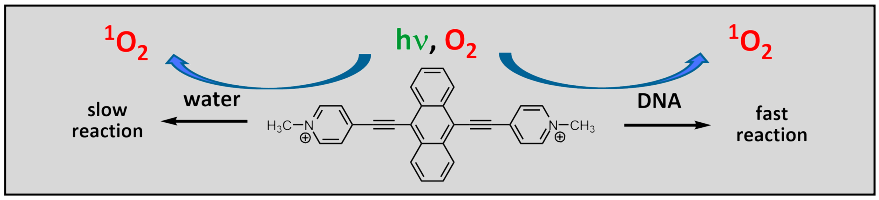

New pyridinium alkynylanthracenes are capable to generate singlet oxygen upon irradiation with green light only, when bound to polynucleotides by intercalation, whereas they slowly decompose when irradiated in water showing poor sensitization activity. Enhanced sensitization activity is observed upon interaction with AT but not GC base pairs. This makes them interesting for applications, where singlet oxygen has to be generated with local control.